Research paper

Stability monitoring method of UHPC spherical hinge horizontal rotation system

Jiawei Wang[1], Bing Cao[2], Bo Huang[3]

Abstract: As the spherical hinge in the bridge swivel structure bears huge vertical pressure, the material and its structural load-bearing capacity are therefore highly-required. In the latest research, the ultra-high performance concrete material is applied to the spherical hinge structure and the author of this article has conducted a detailed study on the mechanical properties and failure mechanism of this structure; however, there is still no real bridge application at present. In order to ensure the stability of the structure, based on an actual project, this research proposes a monitoring method for the stability of the UHPC spherical hinge horizontal rotation system, i.e., using theoretical calculations and numerical analysis methods. Besides, the mechanical characteristics of the bridge during the process of rotation are predicted, and the monitoring data of the stress of the UHPC spherical hinge, the bending moment of the pier bottom, as well as the acceleration time history of the cantilever beam end are made a comparison to judge whether the rotating posture of the structure is stable. The results show that UHPC spherical hinge features high strength and will not cause axial damage; also, the horizontal rotation system will not cause the unstability due to wind-induced vibration and structural self-excited vibration. Briefly concluded, the theoretical model is basically consistent with the measured data, i.e., the mechanical properties of the structure can be accurately predicted.

Keywords: UHPC spherical hinge, bridge swivel construction, construction monitoring, vibration monitoring, wind-induced vibration

[1]PhD., Eng., Anhui Polytechnic University, School of Architecture and Civil Engineering, Wuhu City, Beijing Middle Road, China, e-mail: wjw526@126.com, ORCID: 0000-0002-1263-3150
[2]PhD., Eng., Anhui Polytechnic University, School of Architecture and Civil Engineering, Wuhu City, Beijing Middle Road, China, e-mail: caobing.0427@163.com, ORCID: 0000-0002-6532-5151
[3]PhD., Eng., Anhui Polytechnic University, School of Architecture and Civil Engineering, Wuhu City, Beijing Middle Road, China, e-mail: huangbo@ahpu.edu.cn, ORCID: 0000-0002-7979-1997

1. Introduction

During the construction of large-span rotating bridges, effective construction monitoring is required to ensure that the structural system is in a balanced state to complete the rotating construction. The country that first applied the control theory of the construction process to actual projects was Japan. In 1980, a construction monitoring system was established for a continuous prestressed concrete beam to test the stress and deformation data of key parts of the bridge. Through the analysis and processing of the measured data, the data is sent back to the monitor for structural calculation, and finally the measured value and the calculated value are compared and evaluated and then sent back to the construction site for control during the construction phase [1, 2]. Since then, relevant research has been carried out on the control of structural stress and the setting of pre-camber [3–8], and the industry has begun to study bridge monitoring technology. Then in the 1970s, the Grey System Theory began to be gradually applied to the construction monitoring of continuous rigid frame bridges. In the aforementioned part, monitoring during the horizontal rotation process includes bridge weighing test, calculation and control of construction rotation speed, calculation and control of wind load, stress monitoring of the girder, as well as bridge piers and spherical hinges, etc.

Presently, there have been many reports on the research of UHPC spherical hing, which mainly focus on the mechanical properties and strengthening methods of the spherical hinge, as well as the seismic characteristics of the spherical hinge [9–11]. However, the main methods of the current researches are small-scale test, finite element simulation analysis method. And there is no report on the application of UHPC spherical hinge in real bridge. In order to obtain the force of the structure in the actual project and ensure the safety of the bridge, this research carried out real bridge monitoring on a continuous rigid frame swivel bridge with UHPC spherical hinges. In the research, the force status of the UHPC spherical hinge during the rotation process was tested, the force status of the structure through theoretical calculations predicted; besides, the dynamic response of static wind and pulsating wind to the structure were predicted via the test of the wind speed data at the bridge site. The accuracy of the prediction model is verified by comparing the measured values of the stress and acceleration with the predicted results.

2. Project overview

The test supporting project is a single-width variable-beam high continuous rigid frame bridge with a span of 2×62 m and a maximum cantilever length of 62 m on one side. The girder adopts single box three-chamber inclined web box beam. The top plate of the box girder is 21.3 m wide, the cantilever width of the flange plates on both sides 3m wide, the end thickness of the cantilever plate 20 cm, and the root thickness is 50 cm. The thickness of the top plate of the box girder at the middle fulcrum is 70 cm, and that of the bottom plate is 190 cm. The side fulcrum has a top plate; its thickness reaches 55 cm and the thickness of the bottom plate is 55 cm. The height of the beam along the bridge changes by quadratic

parabolic; when the beam height of the fulcrum reaches 6 m, the beam height of the side span straight section is 2 m, and the swivel weight is about 10,000 t. The spherical hinge structure adopts UHPC. Steel pipe constraints are set on the outside of the spherical hinge and the position of the spherical surface [9] (i.e., the CFST ball joint structure) so as to improve the compressive bearing capacity of the spherical hinge and the flatness between the contact surfaces. The construction site is shown in Fig. 1a to Fig. 1d.

(a) Construction of the girder before swivel

(b) Construction of deck caps and bridge piers

(c) Spherical hinge and ring road construction

(d) Steel pipe supporting foot construction

Fig. 1. Construction site of the background engineering

3. Construction monitoring plan and test method

3.1. Measuring point layout

A total of 2 cross-sections and 8 stress measurement points are set up at the stress measurement points of the bridge piers to test the changes in the stress at the bottom of the pier before and after the rotation. The measuring point should be pre-embedded after the pier's longitudinal main reinforcement is tied up and before the concrete pouring of the bridge pier. The measuring point should be treated with necessary protection when the

concrete is poured. The measurement should be carried out at a time when temperature and sunlight exert little effect on the structure; generally it is between 18:00 and 8:00 the next day. The location and number of the measuring points at the bottom of the pier are shown in Fig. 2.
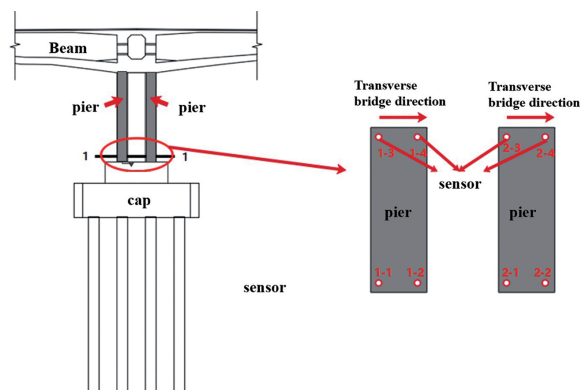

Fig. 2. Arrangement of the measuring points for the pier

UHPC spherical hinge stress measurement points are set with 2 cross-sections and 17 measurement points to test whether the compressive stress of each point before and during the rotation exceeds the limit value of the material's compressive strength. The strain gauge is installed on the positioning steel bar in the lower spherical hinge, and the position of the measuring point is shown in Fig. 3.
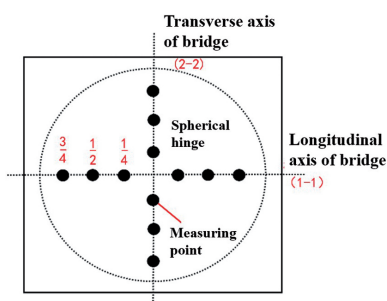

Fig. 3. Arrangement of the measuring points for UHPC spherical hinge

In this construction monitoring, JMZX-215B/RT intelligent string digital strain gauges were selected at the concrete girders and bridge piers. This method is a test method in which the digital strain gauge is embedded in the bridge structure to obtain the strain of concrete by testing the strain of the steel bar. Hence, it is suitable for long-term monitoring. The range is $-1500\sim1500$, and the resolution is 0.1 Hz. The steel string sensor is shown in Figure 3, and the test equipment is a strain tester, as shown in Fig. 4a–4d.

(a) Built-in steel string strain gauge

(b) Concrete strain comprehensive

(c) 941Bseismic vibration pick-up 1

(d) 941Bseismic vibration pick-up 2

Fig. 4. Sensors used in the test

The horizontal rotation angular velocity and acceleration value of the main beam and the vertical vibration acceleration value of the main beam are tested with a 941B vibration pickup, as shown in Fig. 4. A total of 4 cross-sections and 8 measuring points are set. The arrangement of the measuring points is shown in Fig. 5. The 941B vibration pickup is equipped with four gears: acceleration, low speed, medium speed and high speed, which can be selected by the corresponding gear switch. The small size of the sensor can be used for the measurement and monitoring of bridge wind vibration and earthquake, as well as the measurement of ultra-low frequency pulsation, micro vibration and large vibration of the structure.
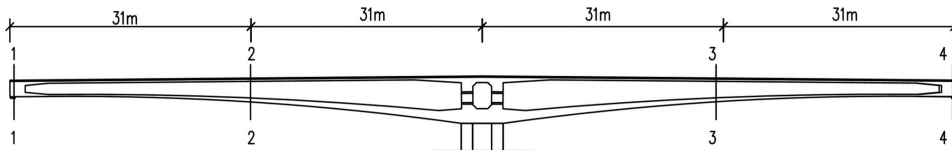

Fig. 5. Measuring points arrangement of speed and acceleration

The sensitivity of the acceleration gear of the vibration pickup is 0.3 (V·s)/m, the maximum range 20 m/s^2; the test frequency range is 0.2~100 Hz, the test accuracy 5×10^{-6} m/s^2; The sensitivity of the low speed gear is 23 (V·s)/m, the maximum range 0.125 m/s; the displacement range is 20 mm, and the test frequency range is 1~100 Hz, the speed test accuracy 4×10^{-8} m/s; The sensitivity of the middle speed gear is 2.4 Vs/m, the maximum range 0.3 m/s, the displacement range 200 mm, and the test frequency range is 0.25~100 Hz, the speed test accuracy 4×10^{-7} m/s. The sensitivity of the high-speed gear is 0.8 Vs/m, the maximum range 0.6 m/s, and the displacement range 500 mm, the test frequency range 0.17~100 Hz, and the speed test accuracy 1.6×10^{-7} m/s. According to the calculations, the test range of the horizontal speed sensor is 0~0.55 m/s, and the range of the vertical vibration acceleration is $0~2.6 \times 10^{-5}$ m/s^2. From the above, the sensor meets the accuracy requirements of the rotating construction process. The installation and on-site monitoring of the sensor are shown in Fig. 6a–6d.
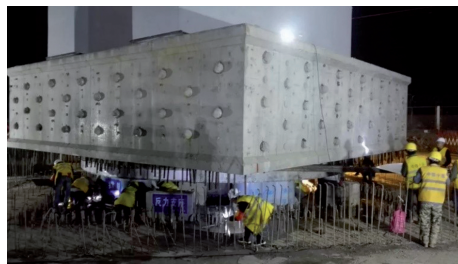

(a) Embedded sensors in various parts of the bridge
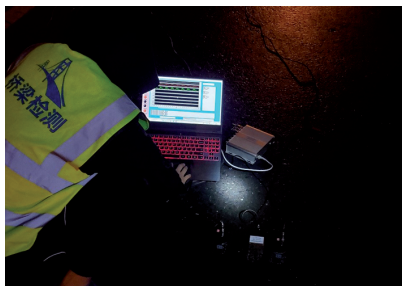
(b) Main beam vibration test

(c) Rotation process

(d) Spherical joint stress monitoring

Fig. 6. Field monitoring chart

3.2. Test of average wind speed at bridge site

The bridge is mainly subjected to wind loads in the process of horizontal rotation, and the bending moment generated at the bottom of the pier will affect the stability of the structure. According to the author's previous research, the static effect of the average wind and the dynamic effect of the pulsating wind can be calculated by testing the average wind speed at the bridge site [12]. The tensile stress value generated by the total effect of the two at the bottom of the pier is used as the control index for the stability monitoring of the bridge during the horizontal rotation process. The test support project is located in the north temperate monsoon zone, bordering the Yellow Sea, with an average annual wind speed of 5.1 m/s. The average wind speed reaches the highest in April of the year at 5.7 m/s. The average wind speed is the smallest in August and September, reaching at 4.5 m/s. And the distribution of wind speed features sea and land breeze. From the above, the construction time of the bridge was set in July when the southeast wind prevails. In order to obtain the actual wind speed at the bridge site, commissioned by the construction party, the meteorological department tested the maximum daily average wind speed of 10 minutes in the 14 days before the bridge rotation construction, as shown in Fig. 7.
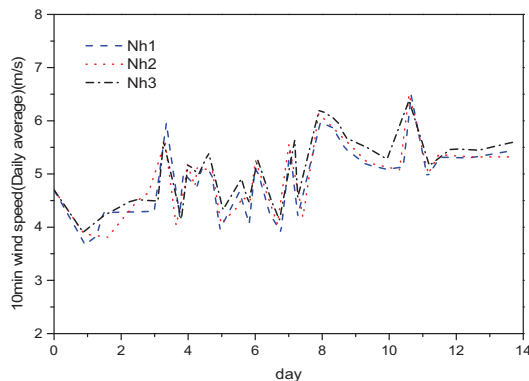

Fig. 7. Measured curve of daily average 10 min wind speed

In the Fig. 7, Nh1~Nh3 are the measurement results of the three instruments, in which the maximum wind speed of 10 min per day is 6.5 m/s and the minimum wind speed is 3.6 m/s. In order to ensure the safety during the turning process, the daily average maximum value of the wind speed in 14 days is selected.

4. Results and discussion

4.1. UHPC spherical joint stress test

According to the layout of the stress measuring points of the spherical hinge, the measuring points are arranged symmetrically along the rotation center of the spherical

hinge, and are arranged at the positions of the center of the sphere (0), 1/4 of the radius of the sphere (1/4R), 1/2R, 3/4R, and R respectively. The two sets of data of UHPC spherical hinge before and during the rotation are shown in Fig. 8. and Fig. 9.

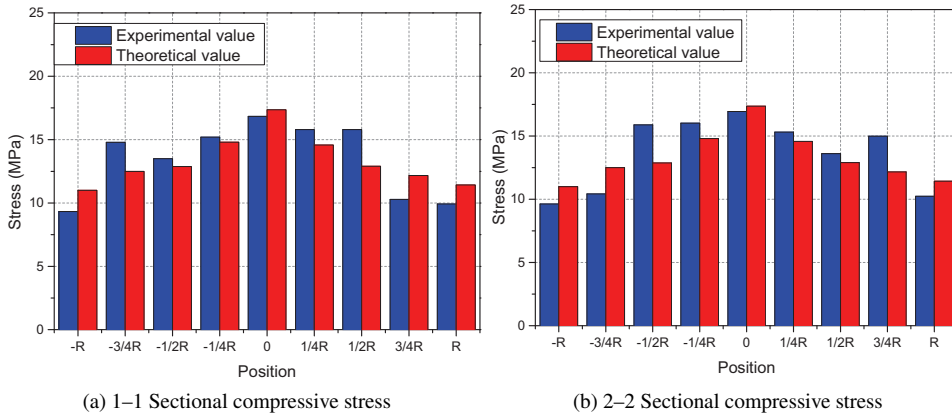(a) 1–1 Sectional compressive stress   (b) 2–2 Sectional compressive stress

Fig. 8. Results of test compressive stress of spherical hinge before rotation

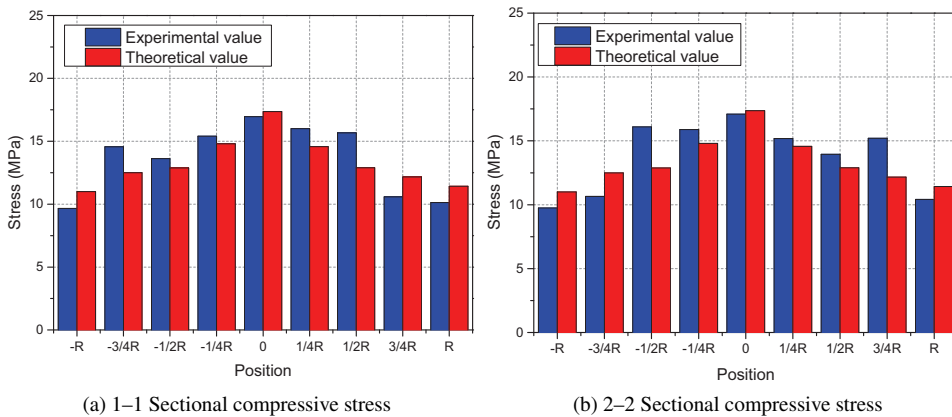(a) 1–1 Sectional compressive stress   (b) 2–2 Sectional compressive stress

Fig. 9. Results of compressive stress test of spherical hinge during rotation

The measured value of the UHPC spherical hinge compressive stress is consistent with the theoretical value. And the compressive stress of the spherical hinge during rotation is below 20 MPa, which meets the requirements of compressive bearing capacity. The compressive stress in the center of the spherical hinge is the largest and gradually decreases to both sides. The measured maximum compressive stress value of the spherical hinge is less than the theoretical value, indicating that the structure has a certain strength reserve and the spherical hinge structure is in a safe operating state. The measured values at local locations are too large, but they are all less than the compressive strength of concrete. The measuring points of section 1–1 are arranged along the longitudinal axis of the bridge, and

the measuring points of section 2–2 along the transverse direction of the bridge. The stress value in the transverse direction is slightly higher, increasing by about 0.1–0.3 MPa, and the manufacturing precision of the spherical hinge is related to the error. In the process of lateral rotation, the upper and lower spherical hinges need to be deformed in coordination, causing a certain stress change. Compared with the static state during the rotation, the spherical hinge compressive stress at the same position has an increase of 0.1–0.2 MPa, but the magnitude of the change is smaller. The results are consistent with the research results are consistent [9, 10], verifying the correctness of the theoretical research. What's more, the construction monitoring results show that the UHPC spherical hinge is always in a lower stress state during the horizontal rotation, and the size of the spherical hinge can be further reduced.

4.2. Pier bottom stress test

In the rotation process, the spherical hinge structure mainly bears the vertical force generated by the dead weight load and the lateral bending moment generated by the average wind and fluctuating wind effects. When the lateral bending moment value is less than the spherical hinge frictional moment, the structure can remain stable under the single-point support of the spherical hinge; when the lateral bending moment value is greater than the spherical hinge frictional moment, the contact between the support structure and the ring will produce support. The reaction force, at this time, is a multi-point support system composed of ball hinges and supporting feet. In the first case, only the lateral unbalanced moment needs to be monitored during the rotation process: when the measured bending moment is greater than the friction moment, the rotation construction should be stopped, and the jack at the support foot position should be lifted to ensure structural stability. When the wind load effect is less than the frictional moment, the structure is in a balanced state under the single-point support of the spherical hinge. At this time, the jack at the support leg is relaxed, and the rotating construction process is continued. In the second case, it is necessary to install pressure sensors at each support foot position, and always keep the support foot stress within the design range during the rotation process. Based on the 14-day average wind speed data at the bridge site, the static and dynamic effects of wind loads are calculated, and the system is in the first case.

4.2.1. Calculation of static wind effect

The effect of static wind adopts the method of Code for Anti-wind Design of Highway Bridges [13], i.e., the static gust wind speed is equal to the product of the static gust coefficient multiples the wind speed at the reference height.

$$V_g = G_V V_z$$

In the above formula, G_V is the static gust coefficient, and V_z is the wind speed at the reference height.

According to the conditions of the test site, the surface category belongs to category B, the rotation radius is 62 m, and the horizontal loading length is 124 m. The value of the

static gust coefficient calculated by linear interpolation is 1.31. The exponential law is used to calculate the average wind speed. In the formula, Z2 equals 16.35 m, and the ground roughness coefficient takes a value of 0.16. The wind speed value at height Z1 above the ground equals 6.5 m/s, Hence, the following results can be obtained:

$$V_{Z2} = \left(\frac{16.35}{10}\right)^{0.16} 6.5 = 7.05 \text{ m/s}$$

$$V_g = G_V V_Z = 1.31 \times 7.05 = 9.24 \text{ m/s}$$

The actual construction time of the test reliance project is less than 2 years. According to the Code for Design of Wind Resistance of Highway Bridges, the wind speed shall be more than 5 years of return period. Besides, consider the actual situation of bridge construction, the design wind speed in the construction phase then finally adopts a return period of 10 years. Also based on the Code for Design of Wind Resistance of Highway Bridges [13], the 10-year wind speed return period coefficient will reach 0.84. So the following formula can be obtained:

$$V_g = 0.84 \times 9.24 = 7.76 \text{ m/s}$$

According to the previous research results, the static wind resistance, lift and torque can be calculated according to the literature [12], and the results of the internal force of the structure under the action of static wind are shown in Table 1.

Table 1. Internal force of each control section under static wind load

Position	Mx/(kN·m)	My/(kN·m)	Mz/(kN·m)	Fy/(kN)	Fz/(kN)
Pier bottom section	786.3	19.4	–	60	71.2
Cantilever root section of main beam	173.4	2085.3	1757.7	55.8	66.2

4.2.2. Calculation of pulsating wind effect

Combine the measured wind speed data wit the time history curve of fluctuating wind load, the buffeting force response of the structure is calculated through time history analysis. Fig. 10 to Fig. 13. show the fitting curves of the downwind direction, vertical wind speed time history, and power spectrum at position 1(#1).

It can be seen from Fig. 10 that the pulsating wind speed in the downwind direction ranges from –5.1 to 4.0 m/s. The maximum wind speed is 5.1 m/s, reaching 78.5% of the basic wind speed. It can be seen from Fig. 12 that the vertical fluctuating wind speed range is –1.5 to 1.4 m/s, and the maximum wind speed is –1.5 m/s, which is 32.3% of the basic wind speed. The pulsating wind in the downwind direction plays a leading role with the average wind speed 2.5 times that of the vertical direction. After being superimposed with the static wind, it produces a dynamic response to the bridge's horizontal rotation system. The average wind speed of the pulsating wind is zero, which does not change the average wind speed value macroscopically, but it exerts some effects on the structure together with the static wind at a certain time interval. It can be seen from Fig. 11 and 13 that the power spectrum
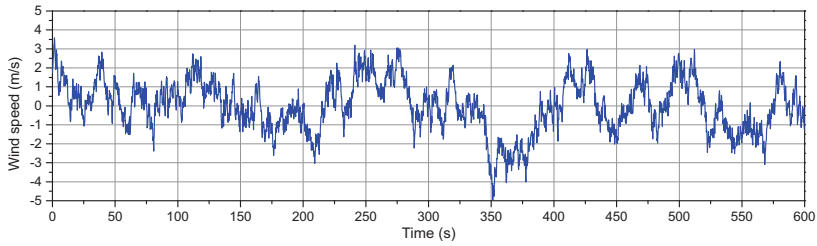
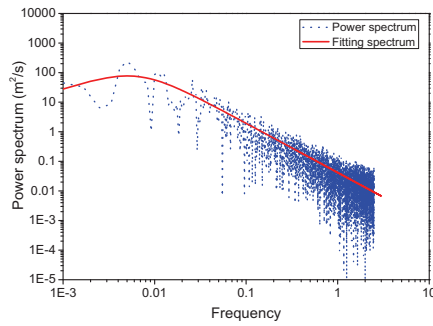Fig. 10. Time history curve of downwind wind speed

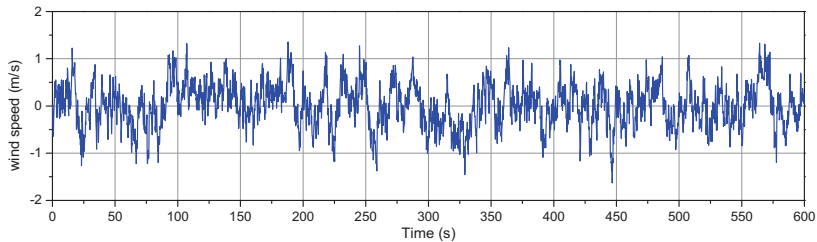Fig. 11. Fitting curve of fluctuating wind power spectrum
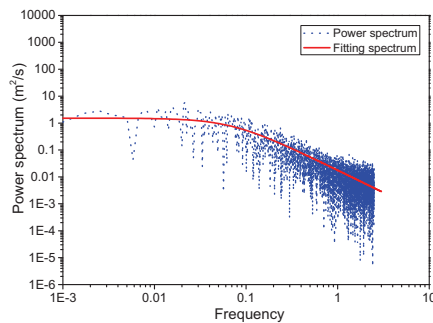

Fig. 12. Time history curve of vertical wind speed

Fig. 13. Fitting curve of fluctuating wind power spectrum

of the pulsating wind has a high degree of fit with the target spectrum. The theoretical calculation results of structural internal forces are shown in Fig. 14, 15 and Table 2.
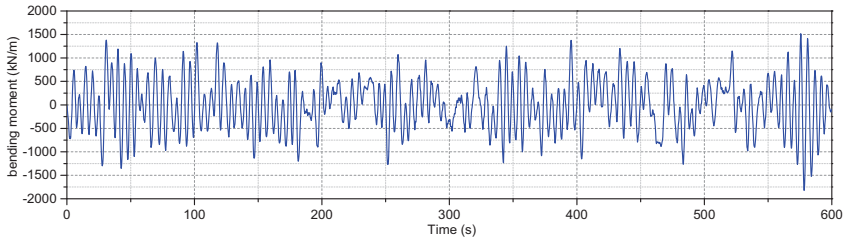

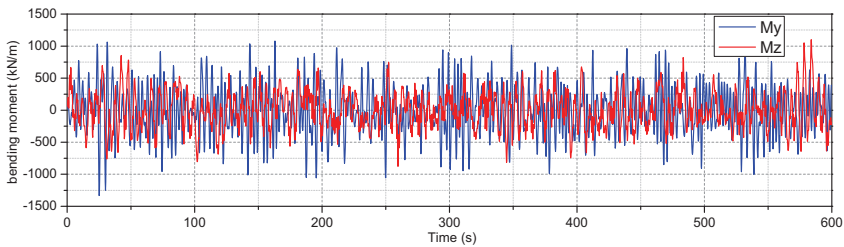Fig. 14. Internal force time history curve of pier bottom

Fig. 15. Internal force time history curve of cantilever root of main beam

Table 2. Theoretical calculation results of internal force and displacement of swivel structure

Position	Results	Static wind effect	Pulsating wind effect	Total effect	Stress/MPa
Pier bottom section	Mx/kN·m	786.3	1822.2	2608.5	0.34
	My/kN·m	19.4	75.7	95.1	-
	Fy/kN	60	321	381	–
	Fz/kN	71.2	395	466.2	–
Cantilever root of main beam	My/kN·m	2085.3	1333.4	3418.7	0.04
	Mz/kN·m	1757.7	1101.8	2859.5	0.05
	Fy/kN	55.8	26.6	82.4	-
	Fz/kN	66.2	31.9	98.1	-

Through the weighing test, the friction moment of the spherical hinge is 5550 kN·m, and the maximum bending moment of the pier bottom is 5217 kN·m, which is less than the friction moment. Therefore, there is no contact between the support foot and the slide during the rotation, reaching the state of single-point support of the spherical hinge. The

stress at the bottom of the pier corresponding to the maximum friction moment of the spherical hinge is 0.34 MPa. The bending moment effect caused by wind load on the girder at the root of the cantilever is small, with the maximum stress at 0.05 MPa, and its influence can be ignored during the construction.

4.2.3. Test results of pier bottom stress

The double thin-walled piers were tested during the construction process, and the maximum stress at the bottom of the pier was shown in Table 3. The positive value is the tensile stress, and the negative value is the compressive stress. The maximum value of the sensor test result equals the measured value during the rotation process. The measured stress value at the bottom of the pier is less than the theoretical value. At the position of 1–1#, the measuring point stress value is the largest, and the converted bending moment of the 1# is 2203 kN·m; the converted bending moment of the 2# pier bottom is 1959 kN·m, Then the maximum lateral unbalanced moment of the spherical hinge structure generated by wind load during the rotation process is 4162 kN·m, indicating that the unbalanced moment is less than the frictional moment of the spherical hinge. The structure is in a stable state under the single-point support of the spherical hinge; thus the structure does not need adjusting by a jack. The rotating construction is completed at one time.

Table 3. Measured and theoretical stress at the bottom of pier in swivel structure

Sensor number	1–1#	1–2#	1–3#	1–4#	2–1#	2–2#	2–3#	2–4#
Theoretical value/MPa	0.34	0.34	–0.34	–0.34	0.34	0.34	–0.34	–0.34
MPa Measured value/MPa	0.27	0.21	–0.24	–0.21	0.24	0.24	–0.24	–0.21

The stability during the rotation process is the main control index, and the stress value at the bottom of the pier directly reflects the lateral stability of the system.

4.3. The vibration test of the grider

The rotating model test shows that the frequency of the first three-order longitudinal bending mode of the girder is the main factor affecting the dynamic stability of the structure. In other words, the construction rotating speed is determined by the relationship between the rotation angular velocity and the frequency. In addition to the flatness of the spherical hinge which will induce structural vibration, the buffeting force of the pulsating wind on the structure will have a greater impact on the structure. Therefore, apart from testing the bending moment at the bottom of the pier during the turning process, it is also necessary to test the vibration acceleration of the main beam to achieve dual control of static and dynamic response to ensure the safety of the horizontal turning process. A total of 4 vertical and 4 horizontal 941-B shock pickups were installed at the beam end and also the position of 1/2L span. The sampling frequency was 200 Hz. The acceleration time history curve of the girder is shown in Fig. 16 and Fig. 17, and the maximum acceleration value and the theoretical calculation result are shown in Fig. 18.
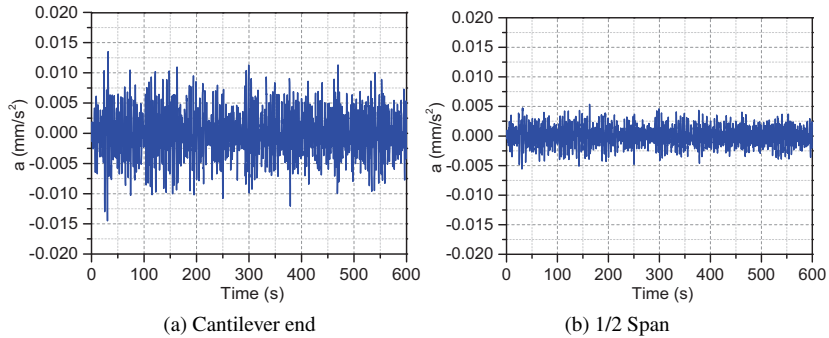
(a) Cantilever end   (b) 1/2 Span

Fig. 16. Vertical acceleration time history curve of main girder

(a) Cantilever end   (b) 1/2 Span
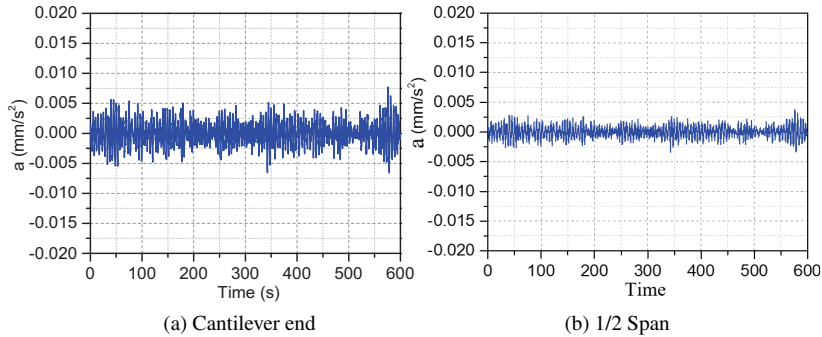
Fig. 17. Transverse acceleration time history curve of main girder

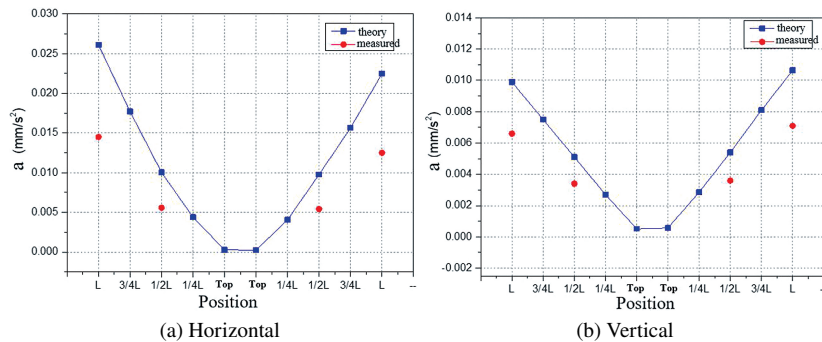(a) Horizontal   (b) Vertical

Fig. 18. Comparison of measured value and theoretical value

It can be seen from Fig. 18. that the actual measured values are all smaller than those obtained from the finite element simulation calculation, which shows the vibration response of the girder is relatively small. Also, the results show that the vibration response of the girder to the bending moment of the pier bottom is less than the friction moment of the

spherical hinge and that the structure is in a stable state under the single-point support of the spherical hinge. Therefore, it can be concluded that the acceleration monitoring results are consistent with the monitoring results of the stress at the pier bottom.

5. Summary

This research carried out construction monitoring of a continuous rigid frame bridge UHPC spherical hinge horizontal rotation system, and obtained the following three conclusions:

1. In the process of horizontal rotation, there is no significant difference between the radial compressive stress value of UHPC spherical hinge is and the static state. Therefore, the influence of the rotation process on the compressive stress of the spherical hinge can be ignored.

2. The stability of the bridge during horizontal rotation is directly related to the force on the bottom of the pier. According to the test results of the 10-min daily average wind speed at the bridge site, a fluctuating wind speed program was established to predict the static and dynamic response of the static wind and fluctuating wind effects to the structure. The results turn out that the prediction model can accurately predict the influence of the pulsating wind effect on the structural stability.

3. The test of the vertical and lateral acceleration values of each section of the girder can help to monitor the influence of self-excited vibration on the stability of the structure. The measured acceleration peak and the theoretical deduction result have a high degree of fit. And the results show that the self-excited vibration of the structure will not cause instability during the horizontal rotation.

References

[1] Y. Zhang, "Construction control and temperature effect analysis of Tianluo super large bridge", Master's thesis, Beijing Jiaotong University, China, 2009.

[2] G. Wang, "Construction control of Long-span Prestressed Concrete Continuous Rigid Frame Bridge Based on Grey Prediction", *Hunan Transportation Technology*, 2019, vol. 45, no. 2, pp. 126–128+174.

[3] J. Miao, "Research on construction monitoring method and closure technology of continuous rigid frame bridge with different thrust stiffness", Master's thesis, Chang'an University, China, 2013.

[4] J. Ma, "Research on monitoring technology for Swivel Construction of T-shaped rigid frame bridge", Master's thesis, Lanzhou Jiaotong University, China, 2018.

[5] Y. Liu, "Study on construction monitoring of rigid frame continuous composite beam bridge", Master's thesis, Changsha University of Technology, China, 2014.

[6] X. Zhang, Y. Zhang, "Discussion on counterweight method of middle span closure section of Prestressed Concrete Continuous Rigid Frame Bridge", *Construction Technique*, 2008, vol. 2008, no. 2, pp. 90–92.

[7] X. Zhang, H. Shu, "Study on closure construction technology of long-span prestressed concrete continuous beam bridge", *Bridge Construction*, 2005, vol. 2005, no. 2, pp. 63–66.

[8] Y. Feng, W. Wu, "Deformation control of cantilever construction closure section of Taolaizhao Songhua River Super Large Bridge", *Journal of Northeast Forestry University*, 2002, vol. 2002, no. 2, pp. 118–120.

[9] J. Wang, Q. Sun, "Experimental Study on Improving the Compressive Strength of UHPC Turntable", *Advances in Materials Science and Engineering*, 2022, vol. 2020, DOI: 10.1155/2020/3820756.

[10]   J. Wang, Q. Sun, "Experimental research on compressive strength of UHPC spherical hinge", *International Journal of Structural Integrity*, 2019, vol. 11, no. 6, pp. 518–537, DOI: 10.1108/IJSI-06-2019-0057.

[11]   Y. Zhang, W. Zhang, "On ultra high performance concrete", *Material Guide*, 2017, vol. 31, no. 23, pp. 1–16.

[12]   J. Wang, Q. Sun, "Study on the influence of fluctuating wind effect on the stability of rotating structure", *Journal of China & Foreign Highway*, 2020, vol. 40, no. 6, pp. 98–103.

[13]   National standards of the people's Republic of China, *Code for wind resistance design of Highway Bridge*. People's Communications Press, 2018.